Mohammad Reza Mohammad Shafiee, Mahboubeh Kargar* and Majid Ghashang

Characterization and low-cost, green synthesis of Zn^{2+} doped MgO nanoparticles

https://doi.org/10.1515/gps-2016-0219
Received December 2, 2016; accepted January 24, 2018; previously published online April 12, 2018

Abstract: The synthesis of oxides has a significant role in their improved properties. This is why a green method is used to gain stable oxide nanoparticles. Zn^{2+} doped magnesium oxide (MgO) nanoparticles were synthesized through a green method, extracting *Aloe vera* latex media. The green method has the advantages of being a cost-effective, innocuous, eco-friendly method. Firstly, thanks to the structure of *Aloe vera* latex, its extract has an important role in morphology, and crystal size of MgO structure, which leads to homogenous nanoparticles dispersion. The elliptical particles with ranges from 45 nm to 65 nm were observed by scanning electron microscopy (SEM) and high-resolution transmission electron microscopy (HRTEM). Furthermore, the effect of calcination temperature was investigated, showing that increasing calcination temperature made larger particles with sharper peaks in X-ray diffraction (XRD) analysis. The strain value (ε) and crystallite size by Williamson-Hall (nm), dislocation density, and crystallinity index were evaluated. Finally, energy dispersive X-ray spectroscopy (EDS) confirmed the doping of Zn^{2+} in MgO nanoparticles. Fourier transform infrared (FT-IR) and HRTEM analyses were also used.

Keywords: *Aloe vera* latex; electron microscopy; MgO nanoparticle; nanostructures; Zn^{2+} doped.

1 Introduction

Magnesium oxide (MgO) nanoparticles with large surface area have been investigated comprehensively in various applications, such as in catalysts, catalyst support, hazardous waste treatment, antimicrobial materials, refractory materials, destructive adsorbent for a large number of pollutants, and superconductor materials [1–3].

***Corresponding author: Mahboubeh Kargar,** Department of Physics, Faculty of Sciences, Najafabad Branch, Islamic Azad University, P.O. Box 517, Najafabad, Iran, e-mail: mahboubeh_kargar@yahoo.com
Mohammad Reza Mohammad Shafiee and Majid Ghashang: Department of Chemistry, Faculty of Sciences, Najafabad Branch, Islamic Azad University, P.O. Box 517, Najafabad, Iran. http://orcid.org/0000-0002-7959-6438 (M. Ghashang)

Furthermore, doping is an important parameter used for nanoparticles due to the reformation of physicochemical properties of metal oxide, which has broad applications, namely in optoelectronics, dilute magnetic semiconductors, and photo detectors [4]. Recently, various elements like Fe, Cd, Mn, Ca, and Zn have doped MgO nanoparticles, making significant versatile properties. As a vivid illustration, with Mn doped MgO nanoparticles, the magnetic property changed from diamagnetic to ferromagnetic [5–8].

In addition, the wide range of applications can be affected by the particle size and crystal morphology of particles determined by scientists to concentrate on the synthesis of MgO nanoparticles. Different synthesis methods have been expressed, including thermal evaporation [9], flame spray pyrolysis [10], the sol-gel technique [11], chemical vapor deposition [12], hydrothermal [13], the auto combustion method [8], and the microwave-induced combustion process [3]. Nevertheless, some of these preparation methods are expensive and complicated processes. Moreover, the use of environmentally cancerous chemicals and organic solvents, which are poisonous, leads to large quantities of wastes inserted into water sources and environments [8–13]. To solve these problems, a simple and viable alternative to chemical and physical methods, namely a green method, has drawn attention, employing fungi, actinomycetes, juices, and plant extracts, which are low-cost, non-toxic, and eco-friendly precursors for the synthesis of nanostructures.

Recently, the biosynthesis of MgO nanoparticles has successfully attracted more attention and interest and some green methods have been developed, including the use of ethanolic fruit extracts of *Aloe vera* gel [6], Emblica officinalis [14], Acacia gum [15], and concentrated solar energy [16].

In this paper, an attempt was made to synthesize Zn^{2+}-doped MgO nanoparticles, mainly due to ionic radius – the ionic radius of Mg^{2+} (0.72 A) is similar to that of Zn^{2+} (0.74 A) [17].

This substitution occurs as the result of a green co-precipitation method in the presence of an extract of *Aloe Vera* latex, and then it was investigated with respect to both structural characteristics and morphology. Analyses of the Zn^{2+}-doped MgO nanoparticles were carried out using X-ray diffraction (XRD), field emission

Table 1: Determination of the size of the crystal, strain value, and dislocation density.

Sample no.	Calcination temperature	Strain value (ε)	Crystallite size by Williamson-Hall (nm)	Particle size by SEM	Dislocation density (m^{-2})	Crystalline index
1	600°C	0.0004	46	40	9.9×10^{14}	0.86
2	700°C	0.002	56	45	9.1×10^{14}	0.80
3	800°C	0.001	65	65	7.8×10^{14}	1

SEM, Scanning electron microscopy.

scanning electron microscopy (FESEM), transmission electron microscopy (TEM), energy dispersive X-ray spectroscopy (EDS), and Fourier transform infrared (FT-IR).

2 Materials and methods

2.1 Physical measurements

Phase identification was carried out for the as-precipitated and heat treated samples by XRD and a Rigaku D-max C III (Japan), X-ray diffractometer, using Ni-filtered Cu Kα radiation. FESEM images were obtained on a HITACHI S-4160 (Japan) field emission scanning electron microscope. Compositional analysis was done by EDS (Kevex, Delta Class I, USA). The morphology of the as-precipitated and heat treated samples was observed with a Philips EM208 (Eindhoven, Netherlands) transmission electron microscope with an accelerating voltage of 200 kV. FT-IR spectra were recorded on JASCO, 6300 (Japan) spectrophotometers in the solid phase, using the KBr pellets technique in the range of 3500–400 cm^{-1}.

2.2 Plant material and extraction

Aloe vera (200 g) was washed in running tap water, mixed with ethanol (50 ml) and distilled water (200 ml) and stirred for up to 4 h on the magnetic stirrer at 100–120°C. A small amount of the extract (100 ml) was used for the synthesis.

2.3 Synthesis of Zn^{2+} doped MgO nanoparticles

Pure magnesium chloride ($MgCl_2$) and zinc chloride ($ZnCl_2$) were purchased from Merck Company (Aldrich) and were used without further purification. Zn^{2+} doped MgO nanoparticles were prepared by the following experimental progression: first, 9.5 mmol of $MgCl_2$ and 0.5 mmol of $ZnCl_2$ were selected and dissolved in 200 ml of distilled water under magnetic stirring. The mixture of 100 ml of extractive *Aloe vera* leaves with 20 ml ammonia was added to the solution under constant stirring in a dropwise manner for ~2 h to gain a homogenous mixture. The obtained mixture was stirred at room temperature for 15 min. The resultant precipitates were filtered, washed with distilled water and absolute ethanol and then dried at room temperature. Moreover, calcination temperature was chosen according decomposition temperature of precipitation such as $MgCl_2$, $ZnCl_2$, and burning *Aloe vera* latex completely [18]. The precipitates were then calcined slowly up to 600°C, 700°C, and 800°C in an

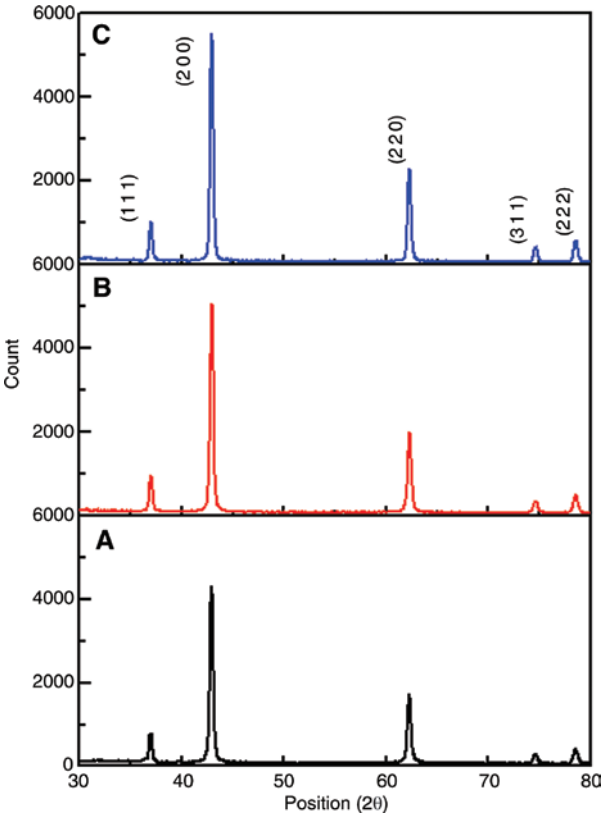

Figure 1: The X-ray diffraction (XRD) patterns of Zn^{2+} doped MgO nanoparticles calcinated at: (A) 600°C, (B) 700°C, and (C) 800°C.

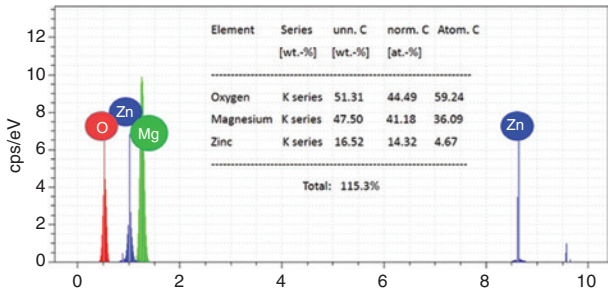

Figure 2: Energy dispersive X-ray spectrums after calcination at 800°C.

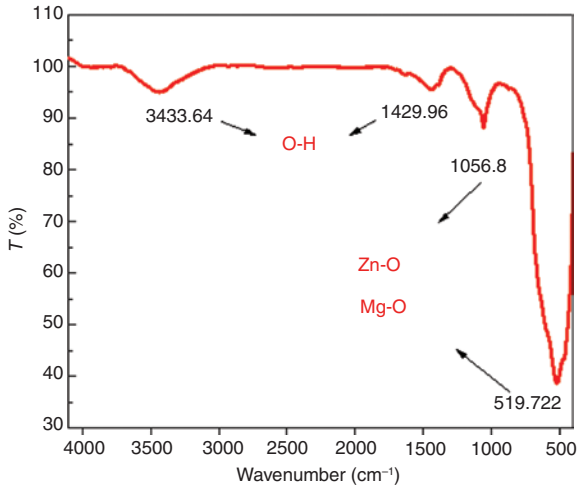

Figure 3: Fourier transform infrared (FT-IR) spectra of Zn^{2+}-doped in MgO nanoparticles after calcination at 800°C.

electric furnace using alumina crucibles and were maintained at the stable mentioned temperature for 3 h. After calcination, the obtained powder of the products was stored in airtight container for further analysis. All of the samples are shown in Table 1.

3 Results and discussion

The Zn^{2+} doped MgO nanoparticles were synthesized via a green co-precipitation method with extract of *Aloe vera* latex as a stabilizer and capping agent to control the crystal growth of nanoparticles. The green co-precipitation method is an economical, non-toxic method which generally leads to the formation of uniform nanostructures.

The correct crystallinity corresponding to that of a single-phase cubic structure (space group $Fm\bar{3}m$), with lattice parameters a = 4.2160Å (JCPDS 087-0651), which is

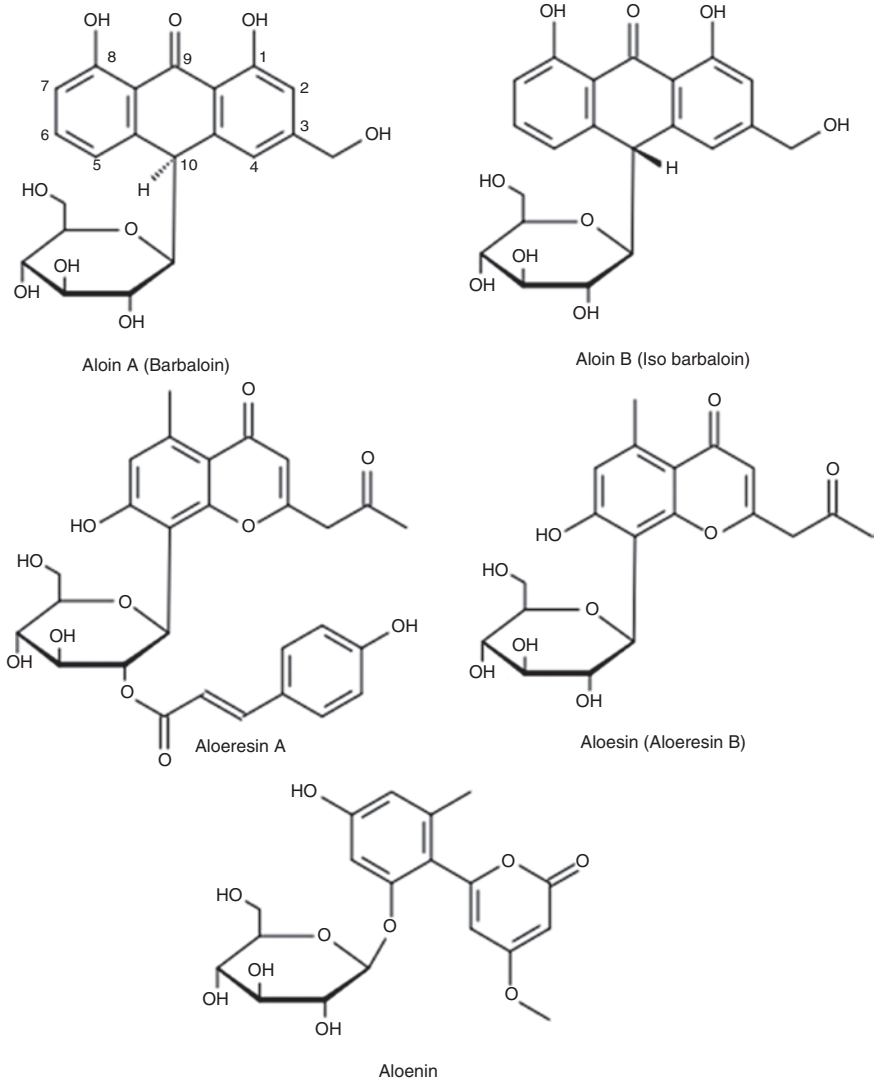

Figure 4: Chemicals present in latex prepared from *Aloe vera* [23].

represented in Figure 1, was observed in the XRD pattern of powders. Overall, the diffraction pattern can show a peak broadening, owing to the effects of particle size and strain factor by using the slope of the Williamson-Hall plot [19]:

$$\beta_{tot}\cos\theta = 4\varepsilon\sin\theta + \frac{k\lambda}{L}. \quad (1)$$

Based on the powder diffraction peak broadening, the strain values (ε) are less than 0.01, due to chemical synthesis and crystalline size of MgO nanoparticles presented in Table 1, confirming that the greater the calcination temperature is, the higher the crystalline size and the better the crystals growth will be. The sharp peaks demonstrate high crystalline size with no indication of any detectable secondary phases. In other words, Zn has been doped in the structure of MgO, albeit it cannot be seen in the XRD pattern. Putting the crystalline size (according to the Debye-Scherrer formula), lattice constant a and width of a diffraction peak at half maximum intensity β into the following equation [20]:

$$\delta = \frac{15\beta\cos\theta}{4aD}, \quad (2)$$

the dislocation density (δ) in the samples was calculated to be around 8.9×10^{14} in Table 1. It is agreed that a larger dislocation density implies a greater hardness in the nanoparticles, because of increasing grain boundary in the sample caused by a decrease in the grain size, preventing the movement of a dislocation by the others at the grain boundaries [21].

EDS analysis was selected to examine the chemical doping of Zn in MgO nanostructures after calcination at 800°C (Figure 2). Characteristic peaks for Zn, Mg, and O in the sample and any trace of the other additives or pollutions are observed. It is shown that the atomic ratio of Mg to Zn in the synthesized samples is about Mg:Zn = 0.907:0.093. $Mg_{0.907}Zn_{0.093}O$ nanoparticles confirmed the amount of Zn in comparison with XRD results.

Additional study of Zn^{2+} doped MgO nanostructures, after calcination at 800°C (Figure 3), shows that the thermal treatment results in the essential disappearance of the IR absorption. Peaks related to the hydroxyl groups of adsorbed water on the surface of MgO nanoparticles were observed at 3430 cm^{-1} and 1429 cm^{-1}. They are respectively related to the stretching and bending vibrations of the absorbed water on the surface of the samples during the handling to record the spectra, because nanoparticles have mixed with KBr [22–24]. The peak at 1056 cm^{-1} indicates the formation of ZnO. A peak at 51 cm^{-1} is attributed to Zn-O and Mg-O bending and stretching vibration of the $Mg_{0.907}Zn_{0.093}O$ sample [25–27].

In this study, extractive *Aloe vera* latex was used as an efficient controlling agent of size and morphology. Four major C-glycosyl constituents in the *Aloe vera* latex are aloin A, aloin B, aloesin, and aloeresin A, shown in Figure 4. The presence of relatively permanent benzene

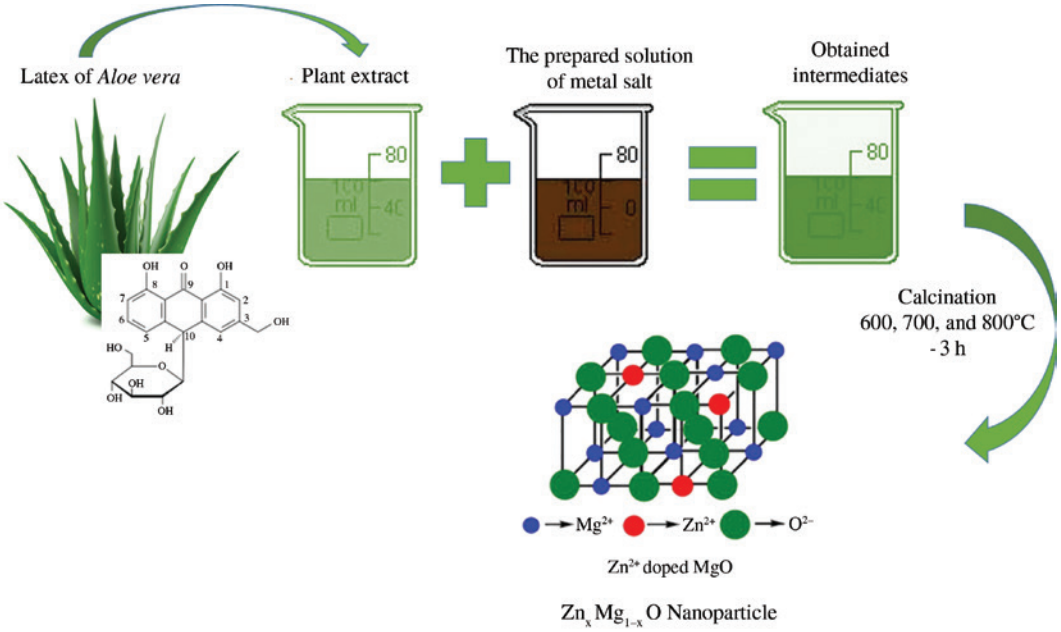

Figure 5: Schematic of effect of C-glycosyl constituents in the *Aloe vera* latex in synthesis of Zn^{2+} doped in MgO nanoparticles.

rings in all of these compounds was controlling and most likely responsible for uniform shapes and sizes of the ensuing discrete nanoparticles [28–30]. A schematic diagram illustrating the effect of glycosyl from extractive *Aloe vera* latex is shown in Figure 5.

The morphology and particle size distribution of the as-prepared samples were investigated using the FE-SEM technique, as shown in Figures 6 and 7. FE-SEM images of the as-prepared nanoparticles using 100 ml of *Aloe vera* extract latex, being calcined at various temperatures of 600°C, 700°C, and 800°C are shown in Figure 6. Nanoparticles were distributed in a homogenous and uniform spherical-shape manner. In other words, they grew radially from the nucleation points on the surface of the aggregated nanoparticles. Segregation of nanoparticles via growth of regular crystalline grains during synthesis is observed, which may lead to greater availability of active sites. Based on Figure 7, with an increase of calcination temperature, the particle size distributions increased in the range of 30–65 nm, thanks to green synthesis. In fact, the C-glycosyl compound in *Aloe vera* extract latex in synthesis advances the growth of particles and prevents agglomeration or micro size structure [6, 31].

TEM images, high-resolution TEM (HRTEM) images, and selected area of electron diffraction of the Zn^{2+} doped MgO nanoparticles after calcination at 700°C are shown in Figure 8. Clearly, in Figure 8A and B it could be seen that the particles have an elliptical shape with diameters of 45–68 nm, and particle distribution is uniform, which is nearly equal to particle size in FESEM images and XRD data. Based on Figure 8C, the lattice fringes between the two adjacent planes is 0.24 nm, which corresponds to the

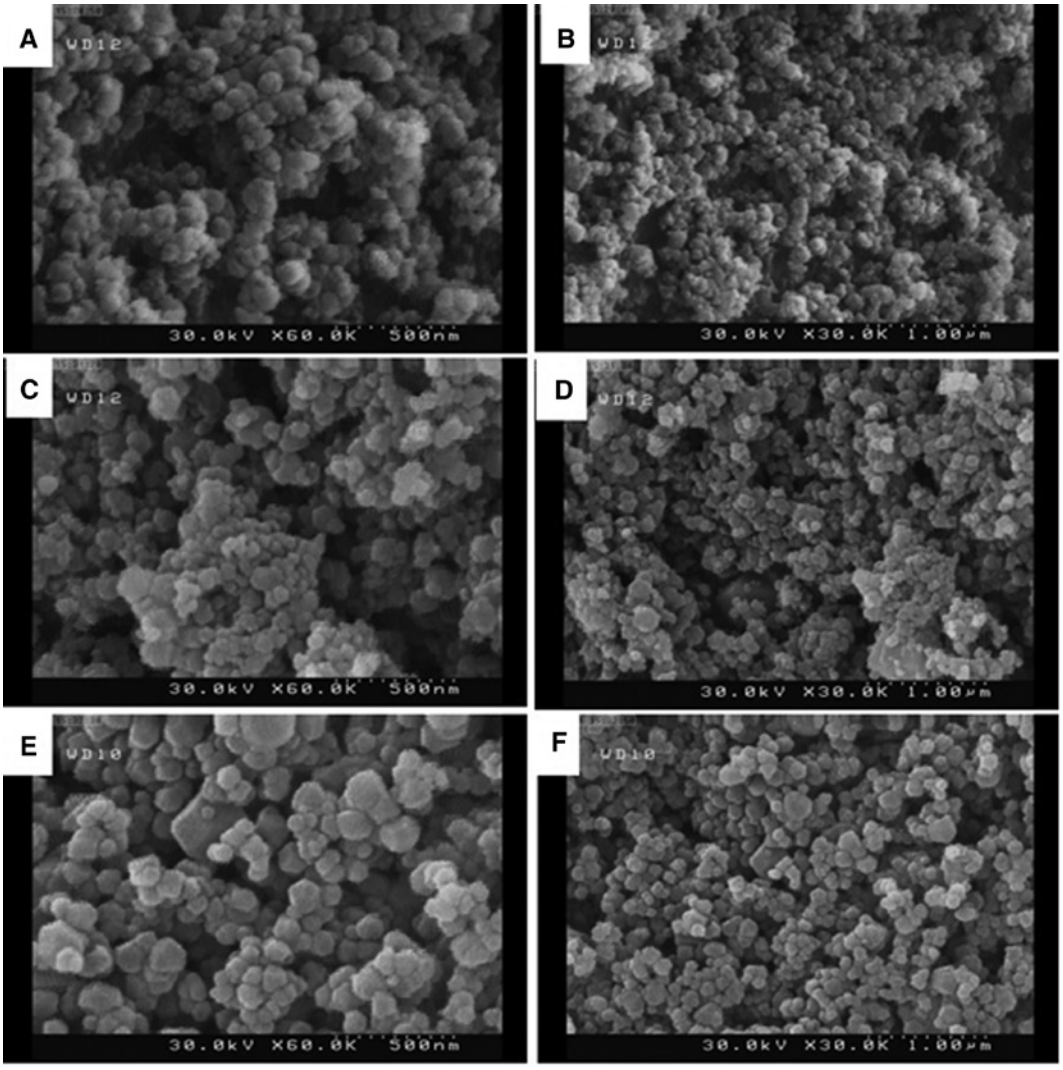

Figure 6: Field emission scanning electron microscope (FESEM) images of of Zn^{2+} doped MgO nanoparticles with two magnitude that calcinated at: (A) and (B) 600°C; (C) and (D) 700°C; (E) and (F) 800°C.

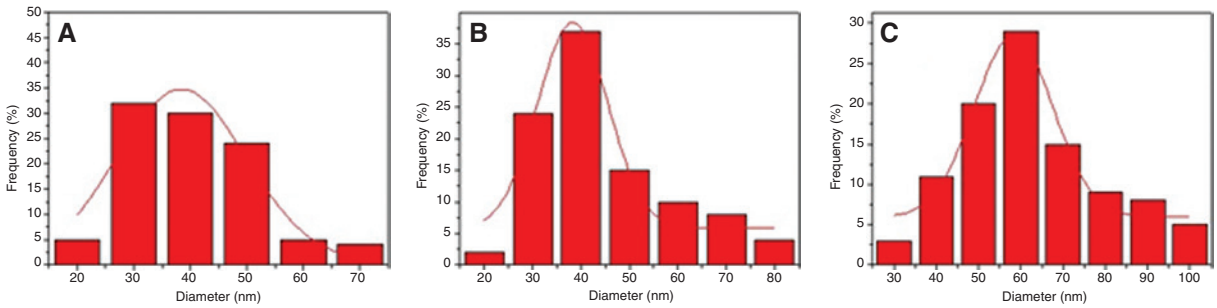

Figure 7: Particle size distribution of Zn^{2+} doped MgO nanoparticles that calcinated at: (A) 600°C, (B) 700°C, and (C) 800°C.

MgO (111) plane, obviously affirming XRD values. The monocrystalline nature of cubic phase MgO nanoparticles is confirmed in Figure 8D. In HRTEM, there was no evidence of the presence of a ZnO crystalline phase, which confirmed Zn^{2+} doped MgO lattice, which was clearly observed in the EDS spectrum of the nanoparticles.

The crystallinity was estimated by comparison of crystallite size as ascertained by TEM/SEM particle size

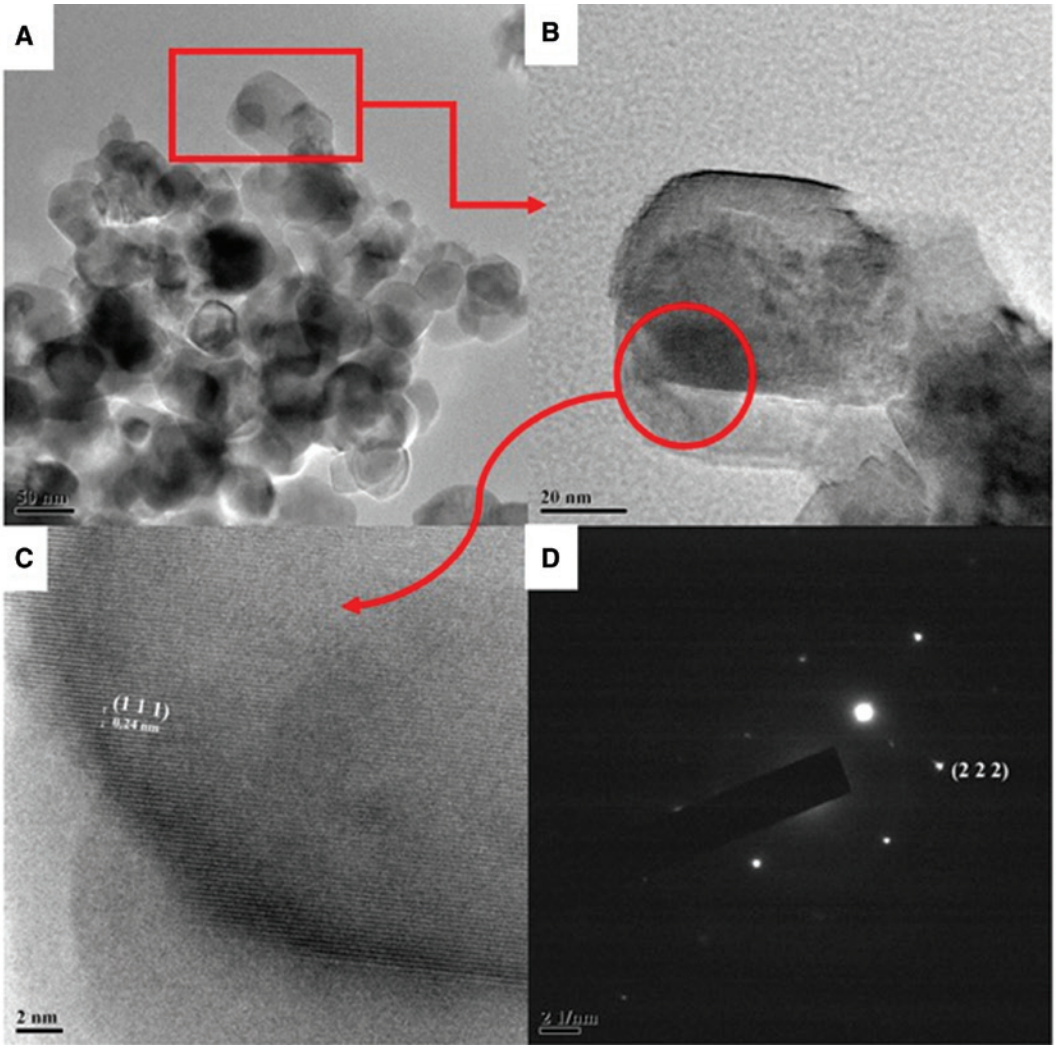

Figure 8: Transmission electron microscopy (TEM) image of of Zn^{2+} doped MgO nanoparticles: (A) and (B) with different magnifications, (C) high-resolution transmission electron microscopy (HRTEM) image, (D) selected area of electron diffraction (SAED) pattern.

determination. Crystallinity index of nanoparticles was estimated using Eq. (3) [32]:

$$I_{\text{cry}} = \frac{D_P(\text{SEM, TEM})}{D_{\text{cry}}(\text{XRD})} \ (I_{\text{cry}} \geq 1.00), \tag{3}$$

where I_{cry} is the crystallinity index, D_P is the average of particle size obtained by SEM or TEM images and D_{cry} is particle size calculated from the XRD data. Table 1 depicts the crystallinity index for all samples that scored near one, confirming a monocrystalline unit that was subsequently confirmed by HRTEM images.

4 Conclusion

In summary, for the first time, Zn^{2+} doped MgO nanoparticles with spherical morphology were synthesized in extract *Aloe vera* latex media, which is a facile, eco-friendly and inexpensive route. Then, their properties were investigated by XRD, EDX, FT-IR, FESEM, and HRTEM techniques. The XRD patterns indicate the structure of MgO without any impurity trace. The EDX analysis confirmed Zn^{2+} has doped in MgO nanoparticles because of its proportion. FT-IR spectra confirmed the formation of MgO nanoparticles. In addition, FESEM analysis showed uniform, homogenous particles with a diameter of around 45–65 nm, due to the green method, which has some advantages such being a non-toxic and low-cost method to obtain nanoparticle uniformly. HRTEM results confirmed the formation of monocrystalline MgO nanoparticles by interplanar spaces. This is in adjustment with XRD results.

Acknowledgements: We are thankful to the Najafabad Branch, Islamic Azad University research council for partial support of this research.

References

[1] Ghashang M, Mansoor SSh, Mohammad Shafiee MR, Kargar M, NajafiBiregan M, Azimi F, Taghrir H. *J. Sulfur Chem.* 2016, 37, 377–390.
[2] Huang L, Li DQ, Lin YJ, Wei M, Evans DG, Duan X. *J. Inorg. Bichem.* 2005, 99, 986–993.
[3] Ouraipryvan P, Sreethawong T, Chavadej S. *Mater. Lett.* 2009, 63, 1862–1865.
[4] Esmaeili E, Khodadadi A, Mortazavi Y. *J. Eur. Ceram. Soc.* 2009, 29, 1061–1068.
[5] Sharma U, Jeevanandam P. *J. Sol-Gel Sci. Technol.* 2015, 75, 635–648.
[6] Azzaza S, El-Hilo M, Narayanan S, Judith Vijaya J, Mamouni N, El Kenz A, Bououdina M, Benyoussef A. *J. Mater. Chem. Phys.* 2014, 143, 1500–1507.
[7] Anilkumar MR, Nagaswarupa HP, Ragabhushana H, Sharma SC, Anantharaju KS, Prashantha SC, Shivakuamra C, Gurushantha K, Vidaya YS. *Spectrochim. Acta. A.* 2015, 149, 703–713.
[8] Kaviyarasu K, Devarajan PA. *Adv. Appl. Sci. Res.* 2011, 2, 131–138.
[9] Stankic S, Diwald O, Sterrer M, Knozinger E, Hofmann P, Bernardi J. *Nano Lett.* 2005, 5, 1889–1893.
[10] Yang Q, Sha J, Wang L, Wang J, Yang D. *Mater. Sci. Eng.* 2006, 26, 1097–1101.
[11] Yi X, Wenzhong W, Yitai Q, Li Y, Zhiwen C. *Surf. Coat. Technol.* 1996, 82, 291–293.
[12] Phuoc TX, Howard BH, Martello DV, Soong Y, Chyu MK. *Opt. Lasers. Eng.* 2008, 46, 829–834.
[13] Hao Y, Meng G, Ye C, Zhang X, Zhang L. *J. Phys. Chem. B.* 2005, 109, 11204–11208.
[14] Kumari L, Li WZ, Vannoy CH, Leblanc RM, Wang DZ. *Ceram. Int.* 2009, 35, 3355–3364.
[15] Ramanujam K, Sundrarajan M. *J. Photochem. Photobiol. B* 2014, 141, 296–300.
[16] Srivastava V, Sharma YC, Sillanpää M. *Ceram. Int.* 2015, 41, 6702–6709.
[17] Patil AB, Bhanage BM. *Catal. Commun.* 2013, 36, 79–83.
[18] Lian J, Zhang C, Li Q, Dickon HL. *Nanoscale* 2013, 5, 11672–11678.
[19] Qiongzhu H, Guimin L, Jin W, Jianguo Y. *J. Anal. Appl. Pyrolysis* 2011, 91, 159–164.
[20] Khorsand Zak A, Wan Haliza, Abd. Majid, Abrishami ME, Yousefi RJ. *Solid State Sci.* 2011, 13, 251–256.
[21] Kargar M, Khoshnevisan B. *Mod. Phys. Lett. B* 2016, 30, 1650148.
[22] Swygenhoven HV. *Science* 2002, 296, 66–67.
[23] Greenwell HC, Jones W, Stamires DN, O'Connor P, Brady MF. *Green Chem.* 2006, 8, 1067–1072.
[24] Mohammad Shafiee MR, Kargar M. *Biointerface Res. Appl. Chem* 2016, 6, 1257–1262.
[25] Kargar M, Alikhanzadeh-Arani S, Bagheri S, Salavati-Niasari M. *Ceram. Inter.* 40, 11109.
[26] Lin Z, Guo F, Wang C, Wang X, Wang K, Qu Y. *RSC Adv.* 2016, 4, 5122–5129.
[27] Etacheri V, Roshan R, Kumar V. *ACS Appl. Mater. Interfaces* 2012, 4, 2717–2725.
[28] Chaitanya Lakshmi G, Ananda S, Somashekar R, Ranganathaiah C. *Int. J. Nanosci. Nanotech.* 2012, 3, 47–63.
[29] Saccù D, Bogoni P, Procida G. *J. Agric. Food Chem.* 2001, 49, 4526–4530.
[30] Hamman JH. *Molecules* 2008, 13, 1599–1616.
[31] Sharrif Moghadassi M, Verma SK. *Int. J. Biol. Med. Res.* 2011, 2, 466–471.
[32] Alikhanzadeh-Arani S, Kargar M, Salavati-Niasari M. *J. Alloys Comp.* 2014, 614, 35–39.